Analysis of Impedance Spectroscopy Measurements of Biological Tissue using the Distribution of Relaxation Times Method

Roberto Giovanni Ramírez-Chavarría[1,2], Celia Sánchez-Pérez[1] and Daniel Matatagui[1]

[1]*Centro de Ciencias Aplicadas y Desarrollo Tecnológico, Universidad Nacional Autónoma de Mexico, AP 10-186, 04510, CD MX, Mexico*
[2]*Facultad de Ingeniería, Universidad Nacional Autónoma de México, 04510, CD MX, Mexico*

Keywords: Biological Tissue, Electrical Impedance Spectroscopy, Distribution of Relaxation Times Method.

Abstract: This work proposes a method for analysing electrical impedance spectroscopy (EIS) measurements of biological tissue in the range of 100 Hz to 1 MHz by means of the distribution of relaxation times (DRT) to evaluate and study the different relaxation time constant involved in electrical response. We numerically analyse different configurations of *RC* circuits and compare the electrical response in time domain by DRT with that of classical EIS representation in frequency domain as Bode plots. Experimental validation of the technique using *RC* circuits, gives an error of less than 1% for the EIS measurement system with respect to theoretical calculation. We present preliminary measurements for WISTAR rat tissue samples of spleen, lung and kidney fixed in formaldehyde solution at 3.8% founding a more detailed occurrence of relaxation mechanism that could provide useful information about the structure and composition of biological tissues in a more precise way.

1 INTRODUCTION

Electrical impedance spectroscopy (EIS) has been widely used to characterize the electrical response of a material by a transfer function that contents information in terms of its electrical properties and mechanisms involved on electrical conduction and polarization. Several EIS techniques can be found in literature for several applications. It has been used in electrochemistry (Barsoukov and Macdonald, 2005) or state of charge in batteries (Osaka, *et al.*, 2012). In biomedical applications different EIS techniques has been developed for the characterization of biological samples as: bone tissue (Ciuchi, *et al.*, 2010), liver tissue in the cases of steatosis disease (Parramon, *et al.,* 2007) and in liver samples of patients with colorectal cancer (Prakash, *et al.*, 2015), as well as gastric tissue for cancer study (Keshtkar, *et al.*, 2012).

In these works, 1 Hz to 1 MHz frequency range for measurements is used because it has been demonstrated that ionic transport of species and polarization of most of the biological tissues occurs at this spectral range for the well-known α and β tissue dispersions (Martinsen, *et al*, 2002).

Impedance is represented by a complex quantity $Z(\omega) = Z' - jZ''$, that is a function of the angular frequency ω. The real part (Z') represents the resistance, while the imaginary component (Z'') represents the reactance. If an oscillating electric current $I(\omega)$ is applied to the material under study one can measure the corresponding voltage drop $V(\omega)$ thus the complex impedance is calculated as:

$$Z(\omega) = V(\omega)/I(\omega) \qquad (1)$$

Commonly, experimental impedance data are fitted at some specific frequencies based on classical EIS models in terms of equivalent electric circuits such as Debye and Cole-Cole (Barsoukov and Macdonald, 2005). Nevertheless, these methodologies need the *a priori* knowledge of some material properties. Alternatively, the distribution of relaxation time (DRT) method has been used for impedance data interpretation (Dion & Lasia, 1999), commonly used in electrochemistry (Saccoccio, *et al.*, 2014). Its main goal is to identify relaxation times from EIS measurements, and as a result, a time scale representation of the complex impedance, can be obtained.

EIS measurements for biological tissue can give out information about its structure and composition,

nevertheless, data interpretation represents a challenge because of the inhomogeneous nature of the tissue, thus several relaxation mechanisms are involved. In this work, we propose the application of DRT method to better analyze the electrical response of formaldehyde fixed biological tissues from EIS measurements in the range of 100 Hz to 1 MHz.

2 THEORETICAL BACKGROUND

Studying biological tissues over a broad frequency range can contain information about their electrical properties revealing their physiology. As discussed in (Martinsen, *et al.*, 2002) a biological tissue can be represented in terms of an equivalent electrical circuit, consisting of an electrode-tissue contact resistance R_∞ in series with a parallel resistive-capacitive representation of a cell, where the extracellular material acts as a resistor (R) and the cellular membrane as a capacitor (C). The inhomogeneity nature of a tissue implies a number n of such RC circuits connected together in series as represented in Figure 1. Thus, according to these electrical behaviour, multiple relaxation times appears, each one associated to the nth circuit, or material.
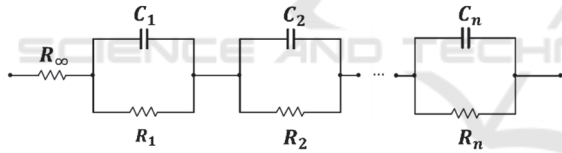

Figure 1: Equivalent electric circuit for a biological tissue.

In circuit theory, a RC circuit is described in terms of the transfer function $H(j\omega)$, according to,

$$H(j\omega) = \frac{1}{1 + j\omega\tau} \tag{2}$$

where $\tau = RC$, represents the constant time of the circuit. So, the physical relaxation time can be related with the constant time of the equivalent circuit associated to a certain material. The characteristic frequency of this circuit $f_0 = 1/2\pi\tau$, represents a maximum of the reactance Z'' on a Bode plot.

2.1 DRT Method

Experimentally, if the frequency related impedance data are measured on a logarithmic scale (Macutkevic, *et al.*, 2004), the equivalent impedance of the circuit shown in Figure 1 is,

$$Z_e(\omega) = R_\infty + \int_{-\infty}^{\infty} \frac{\gamma(\ln\tau)}{1 + j\omega\tau} d(\ln\tau) \tag{3}$$

where the term $\gamma(\ln\tau)$ is a distribution function that joins up the relaxation times. Using a regularized regression approach (Tikhonov, *et al.*, 1995*)*, $\gamma(\ln\tau)$ can be described as a sum of Dirac distributions $\delta(\ln\tau)$ at N relaxation times (Saccoccio, *et al.*, 2014), under these assumptions a discretized form of γ is given by:

$$\gamma(\ln\tau) = \sum_{i=1}^{N} x_i \, \delta(\ln\tau - \ln\tau_i) \tag{4}$$

with x_i being the ith amplitude of the Dirac function at its correspondent τ_i. Eq. (4) is physically equivalent to having N circuits. Combining Eq. (3) and Eq. (4), the impedance DRT model (Winterhalter, *et al.,*1999) is,

$$Z_{DRT}(\omega) = R_\infty + \sum_{i=1}^{N} x_i \int_{-\infty}^{\infty} \frac{\delta(\ln\tau - \ln\tau_i)}{1 + j\omega\tau} d\ln\tau \tag{5}$$

where Z'_{DRT} and Z''_{DRT} can be extracted by multiplying by the complex conjugate $Z^*_{DRT}(\omega)$.

DRT is estimated by fitting Z_{DRT} against Z_e involving the minimization of:

$$\mathbb{S}(\boldsymbol{x}) = \sum_{i=1}^{N} [(Z'_{DRT} - Z'_e)^2 + (Z''_{DRT} - Z''_e)^2] \tag{6}$$

in order to obtain the vector $\boldsymbol{x}$, this last used to compute the value of $\gamma(\ln\tau)$ in Eq. (4).

In this work, DRT algorithm was implanted on an open source software with special optimization and robust mathematics functions. As a final result DRT analysis is given in terms of the distribution function γ in a time scale plot.

For DRT validation, we simulate three parallel generalized RC circuits separately, including a resistor $R_\infty = 200\ \Omega$ for each one. Next, these three circuits were placed together in series. We performed EIS and DRT analysis for the simulated circuits. In Table 1, we summarize the R and C values used for each circuit and their corresponding theoretical calculation for relaxation time and characteristic frequency.

Table 1: Data for simulated RC circuits.

Circuit	R (Ω)	C (nF)	τ (µs)	f_0 (kHz)
RC_1	200.0	48.0	9.6	17.0
RC_2	100.0	1000.0	100.0	1.6
RC_3	56.0	22.0	1.2	130.0

For cases on Table 1, Bode plots for the calculated values of Z' and $-Z''$ are shown in Figure 2. Also we

consider the case when the three circuits are connected together in series $RC_{123} = R_\infty + RC_1 + RC_2 + RC_3$.
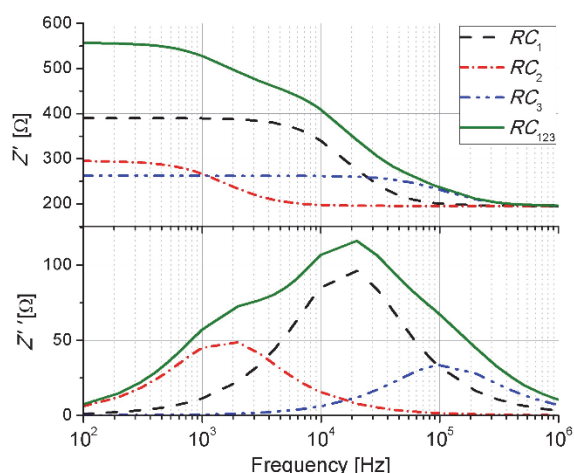

Figure 2: Bode diagram for Z' and Z'' for the simulated RC circuits described on Table 1 and the three circuits placed in series.

One can see that values of Z' are modified as the RC elements are different for each circuit and also the inflection point changes corresponding to the frequency (f_0) at which Z'' has it maximum value. The RC_{123} has a maximum for Z'' at $f_0 = 17.0$ kHz that relates to that of circuit RC_1. Nevertheless, one can expect three values for f_0, but Bode plot representation does not clearly permit to identify all of them.

We utilize the DRT method described above to process EIS data on Figure 2. The distribution function of relaxation times γ is plotted (Figure 3) as a function of the constant time τ for the circuits RC_1, RC_2, RC_3, and RC_{123}.
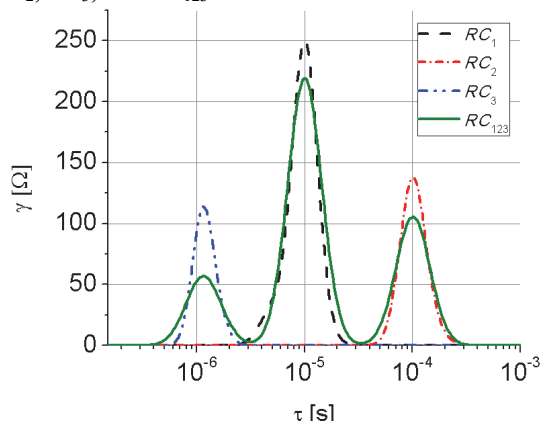

Figure 3: DRT plot as a function of τ for the RC circuits described on Table 1 and the three circuits connected in series.

It can be seen that each maximum is centred at $\tau_1 = 9.3$ μs, $\tau_2 = 100.2$ μs and $\tau_3 = 1.3$ μs, agreeing with theoretical parameters on Table1 with a time scale accuracy less than 5%. Numerical results show that the time domain DRT analysis gives a more precise interpretation of EIS data than that done by frequency domain analysis.

3 MATERIALS AND METHODS

3.1 Animal Tissue Sampling

For tissue samples, a male WISTAR rat, 6 weeks age and 190-220 g weight, was used. After sacrifice, the spleen, lung and kidney were collected whole and put in formalhyde solution at 3.8% for 72 hours.

3.2 EIS Measurement System

We measure the tissue samples using a compact and low cost EIS system, designed by our group of work, capable to perform data processing on line that usually is not included in classical impedance analysers or LCR meters.

The EIS system operates with an alternating current of 400 μA constant amplitude in the range of 100 Hz to 1 MHz for electrical loads from 10 Ω to 10kΩ. Figure 4 shows a scheme of the operation principle in which a 32-bit microcontroller (ARM CORTEX M-4) is the central processing unit with an integrated 16 bit Analog to Digital Converter (ADC) and DSP core.
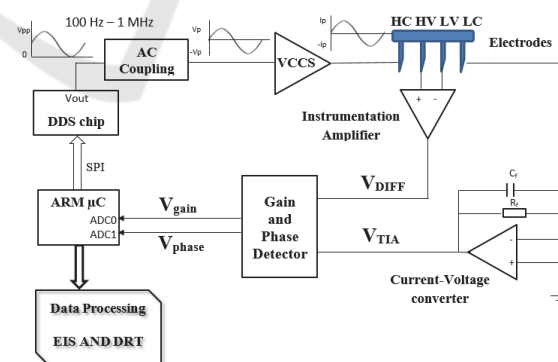

Figure 4: Scheme of the operation principle for the EIS system.

A sinusoidal excitation signal is generated using a digital direct synthesizer (DDS) chip. Two electronic processes are used for AC coupling of the input signal and feeding into a voltage controlled current source (VCCS) unit. The current is injected to the tissue

sample through the high current (HC) electrode and measured from low current (LC) electrode by a low-noise 65 MHz bandwidth transimpedance amplifier (TIA). The TIA output voltage signal (V_{TIA}) is proportional to the measured current. A differential voltage (V_{DIFF}) at the sample is read out by a wide band instrumentation amplifier. Then, the signals V_{TIA} and $V_{DIFF,}$ are compared in a gain and phase detector circuit whose outputs are proportional to the magnitude ratio (V_{gain}) and phase difference (V_{phs}). These two last voltages are digitalized and processed on line in order to obtain the complex impedance, where the impedance magnitude $|Z|$, in ohms, is calculated as follows:

$$|Z| = R_s \cdot 10^{\frac{V_{gain} - 900\text{mV}}{600\text{mV}}} \tag{7}$$

where $R_s = 510\ \Omega$, is the feedback resistor of the TIA circuit. The phase angle θ, in degrees, is obtained by:

$$\theta = -\left(\frac{900\text{mV} - V_{phs}}{10\text{mv/deg.}} + 90\text{deg.}\right) \tag{8}$$

EIS measurements of biological tissue are performed using four stainless steel needle electrodes, fixed on an acrylic support as shown in Figure 5. According to the dimensions of the four electrode array, the geometric factor (Littwiz, et al., 1990) obtained is of $k = 4/5\pi$. Penetration depth of electrodes is 3 mm and it is controlled using a vertical micro positioning stage for accurate measurements.
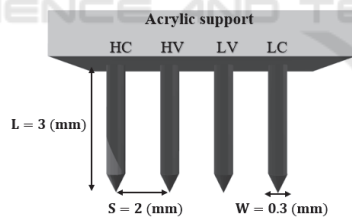

Figure 5: Schematic of the four electrode array used for the EIS measurements.

4 EXPERIMENTAL RESULTS

4.1 RC Calibration Circuit

To validate the EIS system, the RC_{123} circuit was experimentally constructed and measured exhibing an acurracy of 1% for both, magnitude and phase. Once impedance data were collected they were processed using the DRT algorithm. Figure 6 show the DRT results including for comparison theoretical values of Figure 3.
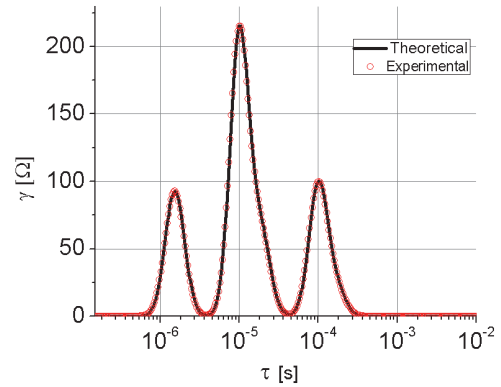

Figure 6: DRT analysis for theoretical and experimental EIS data for the RC_{123} circuit.

DRT results exhibit three peaks, corresponding to each one of the three circuits involved in the RC_{123} circuit, being $\tau_1 = 9.2$ µs, $\tau_2 = 100.2$ µs and $\tau_3 = 1.3$ µs. It can be seen that DRT for experimental data well agree with theoretical values, with a maximum error of 1% among them.

4.2 Biological Tissue Measurements

Electrical impedance measurements were done for WISTAR rat tissue samples of kidney, lung and spleen. After EIS was applied to the tissues, experimental data was collected and then processed with the DRT algorithm. Experimental results are presented in Figure 7.
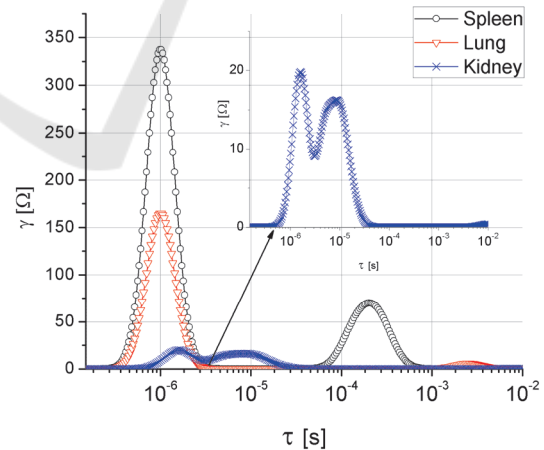

Figure 7: DRT analysis from measured EIS of biological tissue samples.

From DRT analysis of measured tissues, Figure 7 shows the resultant distributions functions versus the time scale for each tissue. For kidney, there are two main peaks, corresponding to the relaxations times, $\tau_{k1} = 1.61$ µs and $\tau_{k2} = 8.29$ µs, it is important to notice

that both are closely separated in the time scale, as shown in the inset plot. For the lung tissue, DRT analysis also exhibits two relaxation processes centred at τ_{l1}=1.0 μs and τ_{l2}=2.0 ms, where clearly, the first one is where the distribution function has more weight and can be taken as the main fingerprint of the lung. Finally, spleen tissue has two relaxation times associated, τ_{s1}=1.0 μs and τ_{s2}=0.2 ms, it can be noted a more weighted distribution around τ_{s1} than that at τ_{s2} as in the case of lung tissue.

5 CONCLUSIONS

This work proposes an alternative analysis to EIS measurements, based on DRT method, which gives a more precise way to found the characteristic electrical processes involved on a tissue, whose are related with its structure and composition. Impedance measurement system exhibits a measurement accuracy less than 1%, whereas DRT algorithm shows a maximum temporal error of 5%. We present preliminary results about distinguishing the relaxation times associated to different tissue samples. Due to the high temporal resolution and accuracy of DRT analysis, it could be applied to characterize the electrical response of biological tissues, that can be useful in the study of some pathologies.

ACKNOWLEDGEMENTS

REFERENCES

Barsoukov, E. and Macdonald, J. R., 2005. *Impedance Spectroscopy: Theory, Experiment, and Applications*. John Wiley & Sons. New Jersey, 2nd edition.

Ciuchi, I. V., Curecheriu, L. P, Ciomaga, C. E., Sandu A. V. and Mitoseriu L., 2010. Impedance Spectroscopy characterization of bone tissues. *Journal of Advanced Research in Physics* 1(1), 011007.

Dion, F. and Lasia, A., 1999. The use of regularization methods in the deconvolution of underlying distributions in electrochemical processes. *Journal of Electroanalytical Chemistry* 475, pp. 28-37.

Keshtkar, A., Slehnia, Z., Somi, M. H. and Eftekharsadat, A. T., 2012. Some early results related to electrical impedance of normal and abnormal gastric tissue. *Physica Medica* 29, pp. 19-24.

Littwiz, C., Rghab, T. and Gaddes, L., 1990. Cell constant of the tetrapolar conductivity cell. *Medicine & Biology Engineering & Computing* 28, pp. 587-590.

Macutkevic, J., Banys, J., and Matulis, A., 2004. Determination of the distribution of relaxation times from dielectric spectra. *Nonlinear Analysis* 9, pp. 75-84.

Martinsen, O. G., Grimnes, S. and Schawn, H. P., 2002. *Interface phenomena and dielectric properties of biological tissue*. Encyclopedia of Surface and Colloid Science, pp. 2643-2652.

Osaka, T., Momma, T., Mukoyama, D. and Nara, H., 2012. Proposal of novel equivalent circuit for electrochemical impedance analysis of commercially available lithium ion battery. *Journal of Power Sources* 205, pp. 483-486.

Parramon D., Erill, I., Guimerà A., Ivorra A., Muñoz, A., Sola A., Fondevila, C., García-Valdecasas, J. C. and Villa, R., 2007. In vivo detection of liver steatosis in rats based on impedance spectroscopy. *Physiological Measurement* 28, pp. 813-828.

Prakash S., Karnes M. P., Sequin E. K., West J. D., Hitchcock, C. L., Nichols, S. D., Bloomston, M., Abdel-Misih, S. R., Schmidt, C. R., Martin Jr, E. W., Povoski, S. P. and Subramaniam, V. V., 2015. Ex vivo electrical impedance measurements on excised hepatic tissue from human patients with metastatic colorectal cancer. *Physiological Measurement* 36, pp. 315-328.

Saccoccio, M., Wan, T., Chen, C. and Ciucci, F., 2014. Optimal Regularization in Distribution of Relaxation Times applied to Electrochemical Impedance Spectroscopy: Ridge and Lasso Regression Methods - A Theoretical and Experimental Study. *Electrochimica Acta* 147, pp. 470-482.

Tikhonov, A., Goncharski, A., Stepanov, V., and Yagola, A., 1995. *Numerical methods for the solution of ill-posed problems*, Kluwer Academic Publishers.

Winterhalter, J., Ebling, D., Maier, D., and Honerkamp, J., 1999. Analysis of admittance data: Comparison of a parametric and a nonparametric method. *Journal of Computational Physics* 153, pp. 139-159.